5596 *Inorg. Chem.* **2009**, *48*, 5596–5598
DOI: 10.1021/ic900538g

Inorganic Chemistry
Communication

Structurally Characterized Iridium(III)-Containing Polytungstate and Catalytic Water Oxidation Activity

Rui Cao, Huiyuan Ma,† Yurii V. Geletii, Kenneth I. Hardcastle, and Craig L. Hill*

Department of Chemistry, Emory University, Atlanta, Georgia 30322. † *Current address: Department of Chemistry, Harbin Normal University, Harbin 150025, People's Republic of China*

Received March 19, 2009

The first structurally characterized iridium-substituted polyoxometalate, $K_{14}[(IrCl_4)KP_2W_{20}O_{72}]\cdot 23H_2O$ [**1**; orthorhombic *Pnnm*, with a = 18.6546(7) Å, b = 19.5192(6) Å, c = 14.8670(5) Å, V = 5413.4(3) Å^3, and Z = 2, final R = 0.0730], is reported. Elemental analysis, X-ray crystallography, and NMR all indicate one Ir atom in each molecule, while IR and electronic absorption spectroscopy, thermal gravimetric analysis, and electrochemistry all indicate its purity in both solid and solution states. Complex **1** is a molecular model of iridium supported on redox-active metal oxides, and aqueous solutions of **1** catalyze oxidation of water to O_2.

Metallic iridium and iridium complexes have long been known as catalysts in several significant organic reactions including C−C bond formation,[1] allylation and vinylation,[2] hydrosilylation,[3] and alkane dehydrogenation.[4] Recently, iridium-containing complexes[5] were found to catalyze the oxidation of water.[6,7] Despite all of these achievements and considerable ongoing iridium chemistry research, however, no crystallographically characterized Ir centers in all-inorganic environments have been reported to date (several noncrystallographically characterized iridium polytungstates are thoroughly documented).[8−14] Some inorganic ligand systems are resistant to hydrolytic and oxidative decomposition as exemplified by a tetraruthenium oxo cluster stabilized by two polytungstate ligands, $[\gamma\text{-}SiW_{10}O_{36}]^{8-}$, that catalyzes the oxidation of water without degradation of the complex.[15,16] Given the importance of iridium complexes in catalytic chemistry and the lack of crystallographically characterized Ir centers in stable inorganic ligand environments, we seek to develop and investigate the chemistry of such species.

Polyoxometalates (POMs), and in particular polytungstates, have many chemical and structural features in common with the redox-active metal oxides used as supports in many important catalytic reactions and processes.[17−20] POM structures and their solubility and stability in solution make them attractive molecular models of metal oxide supports. Furthermore, they are amenable to extensive physicochemical and structural characterization. Defect POMs (derivatives with vacant metal binding sites) are good inorganic

*To whom correspondence should be addressed. E-mail: chill@emory.edu.

(1) Barchuk, A.; Ngai, M.-Y.; Krische, M. J. *J. Am. Chem. Soc.* **2007**, *129*, 8432–8433.
(2) Ngai, M.-Y.; Barchuk, A.; Krische, M. J. *J. Am. Chem. Soc.* **2007**, *129*, 12644–12645.
(3) Calimano, E.; Tilley, T. D. *J. Am. Chem. Soc.* **2008**, *130*, 9226–9227.
(4) Goldman, A. S.; Roy, A. H.; Huang, Z.; Ahuja, R.; Schinski, W.; Brookhart, M. *Science* **2006**, *312*, 257–261.
(5) McDaniel, N. D.; Coughlin, F. J.; Tinker, L. L.; Bernhard, S. *J. Am. Chem. Soc.* **2008**, *130*, 210–217.
(6) Harriman, A.; Pickering, I. J.; Thomas, J. M.; Christensen, P. A. *J. Chem. Soc., Faraday Trans. 1* **1988**, *84*, 2795–2806.
(7) Youngblood, W. J.; Lee, S.-H. A.; Kobayashi, Y.; Hernandez-Pagan, E. A.; Hoertz, P. G.; Moore, T. A.; Moore, A. L.; Gust, D.; Mallouk, T. E. *J. Am. Chem. Soc.* **2009**, *131*, 926–927.
(8) Siedle, A. R.; Newmark, R. A.; Brown-Wensley, K. A.; Skarjune, R. P.; Haddad, L. C.; Hodgson, K. O.; Roe, A. L. *Organometallics* **1988**, *7*, 2078–2079.
(9) Finke, R. G.; Lyon, D. K.; Nomiya, K.; Sur, S.; Mizuno, N. *Inorg. Chem.* **1990**, *29*, 1784–1787.
(10) Lin, Y.; Nomiya, K.; Finke, R. G. *Inorg. Chem.* **1993**, *32*, 6040–6045.
(11) Liu, H.; Sun, W.; Yue, B.; Jin, S.; Deng, J.; Xie, G. *Synthesis and Reactivity in Inorganic and Metal−Organic Chemistry*; Dekker: New York, 1997; Vol. 27, pp 551−566.
(12) Nomiya, K.; Pohl, M.; Mizuno, N.; Lyon, D. K.; Finke, R. G. *Inorg. Synth.* **1997**, *31*, 186–201.
(13) Sun, W.; Yang, F.; Liu, H.; Kong, J.; Jin, S.; Xie, G.; Deng, J. *J. Electroanal. Chem.* **1998**, *451*, 49–57.
(14) Sanders, D.; Howells, A. *J. Undegrad. Chem. Res.* **2008**, *4*, 1–6.
(15) Geletii, Y. V.; Botar, B.; Kögerler, P.; Hillesheim, D. A.; Musaev, D. G.; Hill, C. L. *Angew. Chem., Int. Ed.* **2008**, *47*, 3896–3899.
(16) Sartorel, A.; Carraro, M.; Scorrano, G.; Zorzi, R. D.; Geremia, S.; McDaniel, N. D.; Bernhard, S.; Bonchio, M. *J. Am. Chem. Soc.* **2008**, *130*, 5006–5007.
(17) Pope, M. T.; Müller, A. *Angew. Chem., Int. Ed.* **1991**, *30*, 34–48.
(18) Borrás-Almenar, J. J.; Coronado, E.; Müller, A.; Pope, M. T. *Polyoxometalate Molecular Science*; Kluwer Academic Publishers: Dordrecht, The Netherlands, 2003; p 98.
(19) Hill, C. L. In *Comprehensive Coordination Chemistry−II: From Biology to Nanotechnology*; Wedd, A. G., Ed.; Elsevier Ltd.: Oxford, U. K., 2004; Vol. 4, pp 679−759.
(20) Pope, M. T. *Handbook on the Physics and Chemistry of Rare Earths*; Elsevier: New York, 2008; Vol. 38, Chapter 240, pp 337−382.
(21) Anderson, T. M.; Neiwert, W. A.; Kirk, M. L.; Piccoli, P. M. B.; Schultz, A. J.; Koetzle, T. F.; Musaev, D. G.; Morokuma, K.; Cao, R.; Hill, C. L. *Science* **2004**, *306*, 2074–2077.
(22) Cao, R.; Anderson, T. M.; Piccoli, P. M. B.; Schultz, A. J.; Koetzle, T. F.; Geletii, Y. V.; Slonkina, E.; Hedman, B.; Hodgson, K. O.; Hardcastle, K. I.; Fang, X.; Kirk, M. L.; Knottenbelt, S.; Kögerler, P.; Musaev, D. G.; Morokuma, K.; Takahashi, M.; Hill, C. L. *J. Am. Chem. Soc.* **2007**, *129*, 11118–11133.

Published on Web 05/26/2009

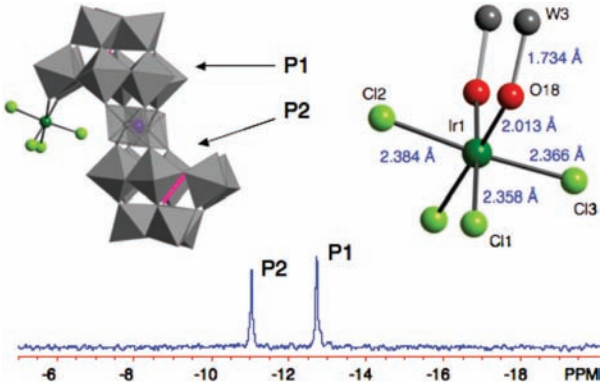

Figure 1. Polyhedral/ball-and-stick representation of polyanion **1a** (top left), $[(IrCl_4)KP_2W_{20}O_{72}]^{14-}$. The WO_6 and PO_4 polyhedra are shown in gray and pink. The Ir, Cl, and K atoms are shown in dark green, light green, and purple, respectively. The top right is the X-ray structure around the Ir in **1a** (Cl2, Ir1, and Cl3 line on a symmetry plane). The ^{31}P NMR spectrum of **1** in D_2O (bottom) shows two peaks at −11.05 and −12.75 ppm, which are assigned to P2 and P1 in the polyanion **1a**, respectively.

ligands, and their properties can be easily and extensively altered. Recent studies indicate that POM ligands are both good σ donors and π acceptors, facilitating stabilization of high-valent transition-metal centers.[21−23] Here, we report the first structurally characterized iridium-containing polytungstate, $K_{14}[(IrCl_4)KP_2W_{20}O_{72}]\cdot 23H_2O$ (**1**), and assess its spectroscopic properties, stability in solution, and catalytic activity for water oxidation.

Attempts to react $IrCl_3$ and $Na_9[A\text{-}\alpha\text{-}PW_9O_{34}]$ always produce colorless all-tungsten complexes: no Ir atoms are incorporated into polytungstates. Hydrolytic degradation of $[A\text{-}PW_9O_{34}]^{9-}$ occurs prior to its reaction with fairly inert d^6 low-spin Ir^{III} centers; thus, we decided to generate the $[A\text{-}PW_9O_{34}]^{9-}$ ligand in situ instead of using its isolated sodium salt. The addition of 1.1 equiv of $IrCl_3$ in water (pH 7.0, adjusted by 1.0 M KOH) to $[A\text{-}PW_9O_{34}]^{9-}$ generated from the reaction of $K_{10}[\alpha_2\text{-}P_2W_{17}O_{61}]$ and K_2WO_4 at pH 6.8, produces a dark-green solution. This solution is stirred at 60 °C for 1 h, and its pH is maintained at 6.8 during this process by the dropwise addition of 1.0 M KOH. Dark-green needles of **1** appear in 2 days if this solution is allowed to stand at ambient temperature. The use of an extra 1 equiv of $IrCl_3$ does not give the diiridium-substituted product (see below and the experiment in the Supporting Information, SI).

The X-ray structure of **1** reveals that the polyanion $[(IrCl_4)\text{-}KP_2W_{20}O_{72}]^{14-}$ (**1a**) is located at the special position with an imposed C_2 axis and a perpendicular symmetry plane. The C_2 axis passes through potassium cation K3 (shown in Figure 1) and W6, and the symmetry plane is defined by Cl2−Ir1−Cl3−P1−W2−K3 (Figure 2). Two symmetry-equivalent $[A\text{-}PW_9O_{34}]^{9-}$ ligands are linked by two $[W^{VI}O_2]^{2+}$ units in an anti configuration. Unlike the other tungsten units in **1a**, the two W6 bridging units both have two terminal oxo groups. The potassium cation located at the center of **1a** (K3) likely stabilizes the overall structure, but this is very difficult to prove.

During our initial refinement, we found that the thermal parameters of the Ir atom and its four Cl ligands are much

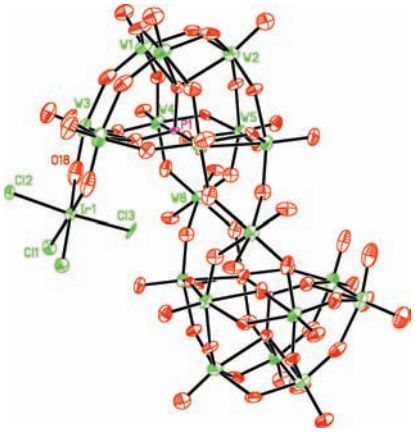

Figure 2. Thermal ellipsoid plot and numbering scheme for polyanion **1a**.

larger than those of the other heavy atoms (Figure S3 in the SI). In addition, there is a large electron density hole (−12.29 e $Å^{-3}$) close to the Ir atom. There are two possible explanations for these anomalous values. First, the dangling $IrCl_4$ unit, which is connected to the polytungstate through two oxo groups (O18), has a structurally proximal distribution of positions, resulting in a spread of their electron densities. Second, the $IrCl_4$ unit is partially occupied. Elemental analysis confirms the second scenario: only one $IrCl_4$ unit is present per polyanion unit. This result suggests half-occupancy of the $IrCl_4$ unit on each of the two symmetric sites. Figure 2 shows the final ellipsoid plot of polyanion **1a**. The crystallographically imposed C_2 axis and the plane of symmetry on a C_s molecule result in the one $IrCl_4$ unit positionally distributed between the two sites.

The Ir−O bond distances are 2.01(2) Å, and the Ir−Cl distances are typical single covalent bonds [2.358(11), 2.384(16), and 2.367(14) Å]. The ^{31}P NMR spectrum (two peaks at −11.05 and −12.75 ppm; Figure 1) is consistent with maintenance of the solid-state structure in solution and confirms that the bulk sample of **1** is pure.

The ability of **1** to catalyze water oxidation was studied. Small amounts of **1** efficiently catalyze the reduction of $[Ru(bpy)_3]^{3+}$ to $[Ru(bpy)_3]^{2+}$ (bpy = 2,2′-bipyridine) in a 20 mM sodium phosphate buffer solution (pH 7.2). In the absence of **1**, the typical reaction time of $[Ru(bpy)_3]^{3+}$ reduction is about 30 min, while in the presence of 3−5 μM **1**, this is shortened to less than 3 min. Cyclic voltammetry (CV) data are consistent with this observation: at a low concentration of **1** (0.03−0.11 mM), a significant increase of the current is observed at a potential corresponding to the oxidation of $[Ru(bpy)_3]^{2+}$ to $[Ru(bpy)_3]^{3+}$ (Figure 3). No such current increase is shown in the control experiments using the polytungstate ligand $[KP_2W_{20}O_{72}]^{13-}$.

On the basis of these findings, we quantified the yield of O_2 in eq 1 by gas chromatography (5 Å molecular sieve column, Ar carrier gas, and thermal conductivity detector). Under unoptimized conditions (1.4 mM $[Ru(bpy)_3]^{3+}$, 0.02 mM **1**, 20 mM sodium phosphate buffer, pH 7.2, 21 °C), the yield was ∼30% (based on eq 1). The low yield of O_2 is consistent with the well-documented catalytic oxidation of bipyridine ligands in $[Ru(bpy)_3]^{3+}$. Because IrO_2 is known to be one of the most efficient catalysts for water oxidation,[6,7] we used $IrCl_3$ as a catalyst in a control experiment: the O_2 yield was

(23) Cao, R.; Han, J. W.; Anderson, T. M.; Hillesheim, D. A.; Hardcastle, K. I.; Slonkina, E.; Hedman, B.; Hodgson, K. O.; Kirk, M. L.; Musaev, D. G.; Morokuma, K.; Geletii, Y. V.; Hill, C. L. *Adv. Inorg. Chem.* **2008**, *60*, 245−272 (Chapter 6).

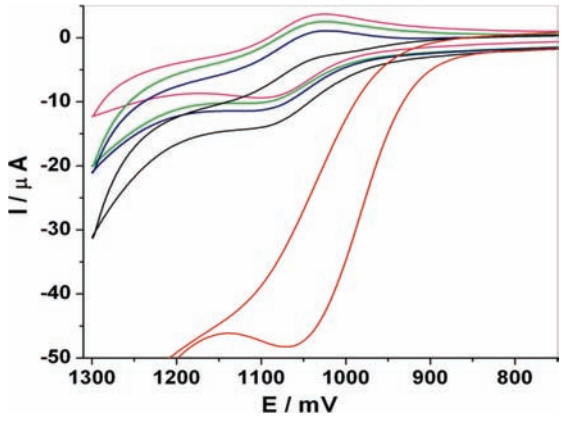

Figure 3. CVs of 1 mM $[Ru(bpy)_3]^{2+}$ solution with different concentrations of **1**: 0, 0.01, 0.03, 0.07, and 0.11 mM, respectively (from top to bottom). Conditions: scan rate 25 mV s^{-1}; 0.2 M sodium phosphate buffer (pH 7.2). Potentials are versus Ag/AgCl.

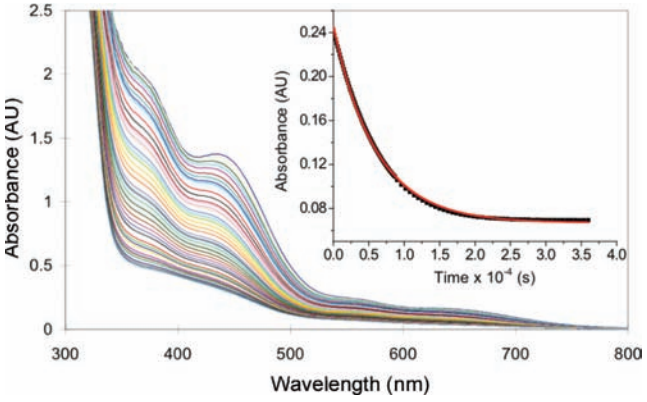

Figure 4. Time profile of the electronic absorption spectra of 1.0 mM **1a** in water (natural pH 6.5) at 25 °C showing the dissociation of $[IrCl_4]^-$ from **1a**. The monomolecular reaction rate constants obtained from fitting of the absorbance at 378, 438, and 556 nm using eq 4 were the same: $k_2 = 1.5 \times 10^{-4}\ s^{-1}$. The example of fitting at 556 nm is shown in the inset: black dots (♦), experimental points; red line, the fitting curve (rms = 0.0029).

almost the same (~38%) under the same conditions. For this reason, we address the stability of **1** in solution.

$$4[Ru(bpy)_3]^{3+} + 2H_2O \rightarrow 4[Ru(bpy)_3]^{2+} + 4H^+ + O_2 \quad (1)$$

The UV−vis spectra of **1** in water change with time (Figure 4). Both ^{31}P NMR and UV−vis studies suggest that the polyanion **1a** dissociates in solution to give $[IrCl_4(H_2O)_2]^-$ and $[KP_2W_{20}O_{72}]^{13-}$ (eq 2). The UV−vis spectrum (350−800 nm) of a 24-h-aged 1.0 mM solution of **1** is almost identical with that of a fresh aqueous solution made from $IrCl_3$. Because the reaction product $[KP_2W_{20}O_{72}]^{13-}$ has a negligible absorbance in this wavelength range (Figure S4 in the SI), this result suggests complete (>99%) dissociation of **1a** in solution in 24 h.

The reaction kinetics were carefully studied. The same half-life ($\tau_{1/2}$) of this dissociation is observed at different initial concentrations of **1** (Figure S5 in the SI; 5600−5800 s), consistent with the reaction rate law in eq 3.

$$[(IrCl_4)KP_2W_{20}O_{72}]^{14-} + 2H_2O \rightarrow [KP_2W_{20}O_{72}]^{13-} + [IrCl_4(H_2O)_2]^- \quad (2)$$

$$[\mathbf{1}] = [\mathbf{1}]_0 \exp(-k_2 t) \quad (3)$$

$$A_t = \varepsilon_1[\mathbf{1}]_0 \exp(-k_2 t) + \varepsilon_2\{[\mathbf{1}]_0 - [\mathbf{1}]_0 \exp(-k_2 t)\} = \varepsilon_2[\mathbf{1}]_0 + \exp(-k_2 t)(\varepsilon_1 - \varepsilon_2)[\mathbf{1}]_0 \quad (4)$$

The first-order rate constant, k_2, was obtained by fitting the experimental data to eq 4, where $[\mathbf{1}]_0$ and $[\mathbf{1}]$ are the concentrations of **1** at time 0 and t, respectively; A_t is the absorbance of the solution at time t at wavelength λ (we used λ = 378, 438, and 556 nm); ε_1 and ε_2 are the molar extinction coefficients of **1** and $[IrCl_4(H_2O)_2]^-$ at λ = 378 (or 438 or 556) nm (determined from freshly prepared solutions of authentic samples). Fitting the data at different wavelengths and different initial concentrations of **1** to eq 4 (Figure 4 and S5 in the SI) gives the same $k_2 = (1.5 \pm 0.1) \times 10^{-4}\ s^{-1}$. Significantly, the same value of k_2 is obtained when **1** decomposes in a 20 mM sodium phosphate buffer (pH 7.2). A good fitting to the exponential law of experimental kinetic curves to high conversions suggests that the reaction products, $[IrCl_4(H_2O)_2]^-$ and $[KP_2W_{20}O_{72}]^{13-}$ (eq 2), do not affect the reaction rate. This conclusion was also confirmed by adding 1.0 mM $K_{13}[KP_2W_{20}O_{72}]$ to the reaction mixture: a small decrease of k_2 from $(1.5 \pm 0.1) \times 10^{-4}\ s^{-1}$ to $(1.2 \pm 0.1) \times 10^{-4}\ s^{-1}$ was in the range of experimental error (Figure S7 in the SI).

The findings that (i) the oxidation of water (eq 1) in the presence of **1a** proceeds much faster than the dissociation of **1a** (eq 2), (ii) both **1a** and $IrCl_3$ (a model complex of the decomposition product of **1a**) show similar activities, and (iii) the POM ligand $[KP_2W_{20}O_{72}]^{13-}$ is inactive to water oxidation argue that intact **1a** could well catalyze water oxidation. However, it cannot be ruled out that under turnover conditions **1a** is much less stable and thus produces a small and undetectable amount of catalytically active IrO_2 nanoparticles.

In conclusion, the first crystallographically characterized Ir-substituted POM is reported. A $IrCl_4$ unit is ligated to the polyanion $[KP_2W_{20}O_{72}]^{13-}$ through two O atoms. Crystalline **1** is pure and stable in the solid state but slowly decays in an aqueous solution. Complex **1** may catalyze the oxidation of water by strong oxidants, such as $[Ru(bpy)_3]^{3+}$.

Acknowledgment. We thank the Department of Energy (Contract DE-FG02-07ER15906) for support of this work.

Supporting Information Available: Detailed synthesis, characterization, and crystallographic studies, including the CIF file of **1**, Figures S1−S9, and Table S1. This material is available free of charge via the Internet at http://pubs.acs.org.